UNIVERSITY OF
BATH

Citation for published version:
Mohammadi, A, Bowen, C, Sadrafshari, S & Yuce, MR 2020, 'Time Domain Multiplexing for Efficiency Enhanced Piezoelectric Energy Harvesting in MEMS', *IEEE Electron Device Letters*, vol. 41, no. 3, pp. 481-484. https://doi.org/10.1109/LED.2020.2965143

DOI:
10.1109/LED.2020.2965143

Publication date:
2020

Document Version
Peer reviewed version

Time Domain Multiplexing for Efficiency Enhanced Piezoelectric Energy Harvesting in MEMS

A. Mohammadi, S. Sadrafshari, C. R. Bowen, M. R. Yuce

***Abstract*—The conversion efficiency of piezoelectric energy harvesters (EH) have been improved by several approaches including frequency up-conversion (FUC) techniques that trigger the high-frequency (HF) piezoelectric resonators using low-frequency (LF) mechanical inputs. This work proposes a new time-domain multiplexing technique to further improve the harvesting efficiency for random mechanical impacts using commercially available microfabrication processes. The FUC is implemented by a slowly moving shuttle beam, which represents the LF mechanical inputs, that triggers the free ends of piezoelectric cantilever beams. Mechanical impacts by the LF shuttle lead to the cantilever beams vibrating at their higher natural resonance frequencies. In the proposed approach, resonators are exposed to the LF mechanical input at unequal distances, which results in sequential HF vibrations. As a result, the HF electrical outputs fit sequentially within the long period of the LF input. Analytical and experimental comparisons support the increased electrical output using time domain multiplexing.**

***Index Terms*— Piezoelectric Energy Harvester, Frequency Up-converter, Micro-electromechanical Systems (MEMS)**

I. INTRODUCTION

Microelectromechanical systems (MEMS) provide a low-cost and highly reliable platform for autonomous and self-powered microsystems to employ a variety of transduction mechanisms and convert different forms of energy into electrical energy [1-5]. Vibration-based EH, using electrostatic [1], electromagnetic and piezoelectric transducers [3, 4], have demonstrated higher energy outputs compared to other mechanisms. Electrostatic transducers require an electric power supply to charge the capacitor plates and electromagnetic transducers suffer from lack of straightforward microfabrication processes due to the need for integrated permanent magnets [6]. Therefore, piezoelectric transducers have gained higher popularity as fully autonomous solutions that use monolithic MEMS processes.

The conversion efficiency of piezoelectric transducers is an optimum for mechanical inputs at the transducer resonance frequencies. However, this frequency can often be much higher than the mechanical vibrations or displacements being harvested, especially for small scale MEMS transducers. As a result, several frequency up-conversion (FUC) mechanical structures have been presented to transfer the energy from low-frequency (LF) inputs to higher frequencies (HF) [2, 5]. Furthermore, meso-scale two-beam impact-based harvesters can extract energy at several resonance frequencies, which increases the EH bandwidth [7]. However, this type of structure is incompatible with existing microfabrication technologies.

The efficiency of linear EH systems with deterministic inputs is independent of the mechanical input and most ambient mechanical excitations exhibit a random behavior, such as force levels with Gaussian distribution [8-10]. In this paper we propose a new time-domain-multiplexing (TDM) method for sequential multi-beam excitation to capture inputs with low amplitude, which may be otherwise wasted in multi-beam systems that expose all the beams simultaneously. The following sections report the analysis, development and experimental validation of the proposed TDM technique in standard microfabrication processes.

II. PROPOSED TIME DOMAIN MULTIPLEXING TECHNIQUE

Fig. 1(a) illustrates the schematic of a piezoelectric EH system with two cantilever beams (Pz_1 and Pz_2) simultaneously exposed to random LF mechanical impacts, such as force. This parallel structure splits the input force between the two beams.

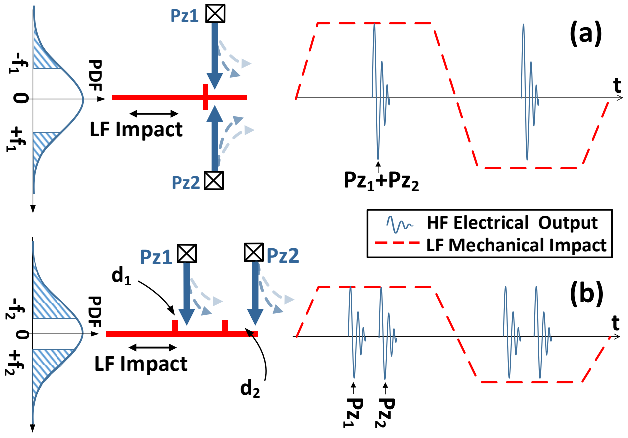

Fig. 1. LF random mechanical input applied to multi-beam FUC, (a) Scenario 1: parallel beams receive mechanical impact simultaneously, (b) Scenario 2: the proposed TDM: mechanical impact is applied sequentially to the beams, $d_2>d_1$.

Dr A. Mohammadi (Corresponding author: am3151@bath.ac.uk), Dr S. Sadrafshari, and Prof. C. R. Bowen are with the Faculty of Engineering, University of Bath, Claverton Down, Bath (BA2 7AY), UK.

Dr M. R. Yuce is with the Department of Electrical and Computer Systems Engineering, Monash University, Clayton, VIC (3800), Australia.

Assuming that the mechanical input exhibits a white Gaussian distribution with zero mean and specified variance, it will only capture forces larger than a certain value, e.g. f_1, as illustrated by the dashed area under probability density function (PDF).

We now introduce a new approach to increase the total output energy by TDM of the LF mechanical input, as shown in Fig. 1(b). In this approach the piezoelectric beams are exposed to the LF input at unequal distances (d_1 - d_2). This allows each beam experience the entire mechanical impact at sequential time instances, i.e. the input triggers only one beam at each time instance, which leads to a smaller input force (f_2) required for triggering the beams in comparison with parallel excitation (Fig 1(a)). Hence, TDM captures input forces available within wider range of magnitudes, as illustrated by the dashed area under PDF, which increase the electrical output for identical mechanical input.

These two scenarios represented in Figures 1(a) and (b) are further analyzed in the following analysis to demonstrate the advantages of proposed TDM technique.

The mechanical strain distribution in response to the applied input to the free end of cantilever beam [5] is given by

$$\xi(x) = \frac{3t_b(l_b - x)}{2l_b^3}\delta_b \qquad (1)$$

where t_b, l_b, and δ_b represent the beam thickness, length and tip deflection, respectively. The open-circuit voltage output of this piezoelectric beam depends on the tip deflection (δ_b):

$$V_{O.C.} = \frac{-d_{31}Yt_e}{\epsilon_{33}}\int_0^{l_b}\xi(x)dx = \frac{-d_{31}Yt_e}{\epsilon_{33}}\frac{3t_b}{4l_b^2}\delta_b \quad (2)$$

where d_{31}, ϵ_{33}, Y, and t_e are transverse piezoelectric constant, dielectric coefficient (relative permittivity), Young's modulus, and the thickness of piezoelectric layer, respectively. The deflected and released beam output voltage consists of damping oscillations with the initial magnitude $V_{O.C.}$. The tip deflection translates to the shuttle input force through the beam stiffness ($f = k\delta_b$). Assuming that the input force has a white Gaussian distribution, the proposed technique will capture the LF forces larger than f_2 in Fig. 1(b) (Scenario 2) compared with a parallel beam structure that only captures forces larger than f_1 in Fig 1(a) (Scenario 1). We now define a function to count the number of LF force inputs that result in output voltages (successful outcomes) versus the number of inputs that are not sufficiently strong to bend and release the beam:

$$N(t,f) = \begin{cases} 1 & f \geq f_1 \\ 0 & f < f_1 \end{cases} \qquad (3)$$

The electrical output is proportional to the total number of successful force inputs obtained by the expected value of N

$$E[N] = \int_{-\infty}^{\infty}\frac{1}{2\sigma^2}e^{\frac{-(f-\mu)^2}{2\sigma^2}}df \qquad (4)$$

where σ represents the variance and the mean $\mu = 0$ for Fig 1. In order to compare the electrical output of the two scenarios in Fig 1, we calculate the integral in (4). Hence, the output voltage increase achieved by TDM of multiple beams, which translates to $f_1 = nf_2$, is proportional to

$$\frac{V_{O.C.2}}{V_{O.C.1}} = \frac{1+\mathrm{erf}(^{-f_1}/_{n\sigma\sqrt{2}})}{1+\mathrm{erf}(^{-f_1}/_{\sigma\sqrt{2}})} \qquad (5)$$

where n represents the number of beams, and *erf* is the error function. This increase depends on the ratio of minimum force needed to release the beam over the variance of input force ($f_1/\sigma = r$). This is shown in Fig. 2 by sweeping the increase in electrical output (5) over n, for different values of r. It should be noted that the higher energy for the larger r values does not essentially translate to larger total energy output because it includes a smaller range of mechanical inputs. This indicates that the approach is particularly attractive for low amplitude harvesting.

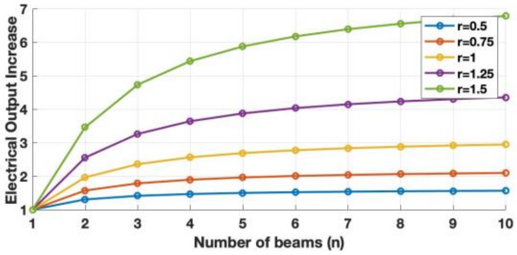

Fig. 2. Electrical output increase achieved by using multiple beams (n) for different minimum force over variance ratio (r).

The proposed technique is implemented in a commercially available microfabrication process (Pz-MUMP) [11], which consists of a piezoelectric layer (AlN) sandwiched between two electrodes. The bottom and top electrodes consist of a 10μm thick Silicon-on-Insulator (SOI) layer and a 500 nm thick metal layer (Al), respectively.

The chip microphotograph is illustrated in Fig. 3(a). The meander shape design reduces the stiffness of these beams and lowers their resonance frequencies. This design ensures that mechanical force generated by the electrothermal actuator is sufficient to bend the beams. Furthermore, this will allow the lateral mechanical input to trigger the transverse mode (d_{31} coefficient) of piezoelectricity in this microstructure. As illustrated in the magnified inset image, see Fig. 3(b), the distance between the sharp shuttle protrusions and the free ends of the beams (d_1 and d_2) are designed to be unequal. In an idle mode, these distances vary from 5μm to 10μm. These distances ensure the shuttle makes contact with only one pair of beams immediately after releasing the previous pair.

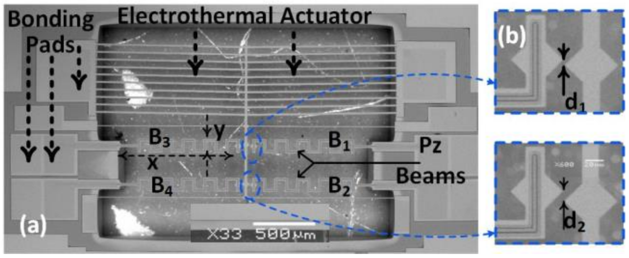

Fig. 3. SEM image of the prototype microchip, (a) meander-shape beams (B_1, B_2, B_3, B_4), electrothermal actuator (x=850μm, y=100μm), (b) magnified image of shuttle protrusions and beam tips (d_1=5μm, d_2=10μm).

III. SIMULATION AND MEASUREMENT RESULTS

The piezo-electromechanical simulations of meander shaped cantilever beams are carried out in Coventorware®, see Fig. 4. The beam 3D model was implemented by supplying the material property database and process steps following the Pz-MUMP manual [6]. The minimum force required to bend and

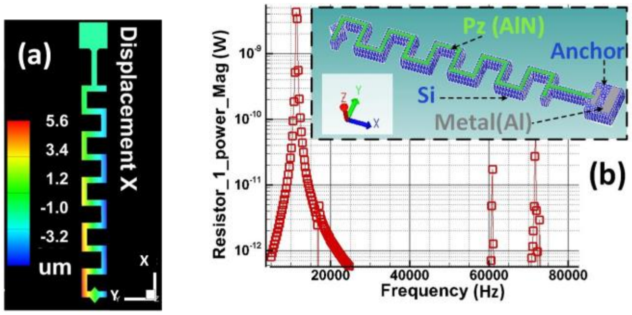

Fig. 4 Finite element analysis, (a) tip displacement in X direction in response to the force in Y direction that pluck the beam, (b) Harmonic balance analysis, the spectrum of power delivered to a 1MΩ resistor.

release the beam is obtained by applying a force vector in the y-direction to the free end of the beam and measuring the displacement. The displacement in the x-direction indicates the force needed to pluck the beam by the shuttle protrusions, see Fig 4(a). This is approximately 0.2mN for a 1µm overlap between the protrusions and beam tips, which is represented by f_2 in Fig. 1(b).

The piezoelectric physics is included for nonlinear steady-state analysis that run for 500 frequencies over 5 kHz~70 kHz, see Figure 4(b). The fixed end is anchored to the substrate and a mechanical input is applied by setting 1 g acceleration in the out-of-plane z-direction. The top and bottom electrodes are connected to a 1 MΩ resistive load. The peak output power is approximately a few nanowatts delivered at the 12 kHz resonance, which triggers the transverse piezoelectric mode.

The application of LF electrical input to the electrothermal actuator moves the shuttle that mimics the LF mechanical inputs [12]. The in-plane impact of LF shuttle triggers the out-of-plane mode shape of resonator, due to its specific geometry of 20µm width and 10µm thickness. The amplified time-domain signals recorded from all piezoelectric beams are shown in Fig. 5(a). The LF signal is a 2 Hz, 3.5 V sinusoidal voltage. The released beams generate HF vibrations at 9900 Hz at their natural resonance frequency; see the inset in Fig. 5(a).

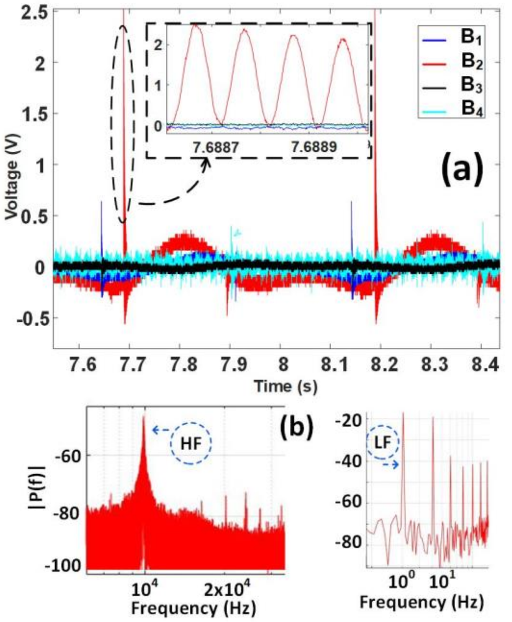

Fig. 5 Measurement results, (a) time domain measurements of voltage outputs from the piezoelectric beams in response to 2Hz LF mechanical input, (b) Power spectrum of B_1 output and LF input and its harmonics

This confirms the ability to achieve FUC from the LF shuttle up to the beam resonance frequency.

In addition, the voltage outputs recorded from piezoelectric beams ($B_1 – B_4$) in Fig. 5(a) show sequential time instances. The design of different spatial distances between shuttle protrusions and the tips of beams (d_1 and d_2 in Fig. 3(b)), results in non-synchronous voltage outputs, which demonstrates the time-domain multiplexing of multiple HF vibrations. Furthermore, in each LF period the shuttle sweeps through each beam twice in opposite directions. These two generate unequal voltage levels depending on the impact point geometries and the beam shapes, which is only visible for B_1 and B_2 on this chip.

The power spectrum of these signals is demonstrated in Fig. 5(b), which shows the resonance of the beam at ~10 kHz and the LF input (at 2 Hz) and its harmonics. The difference between resonance frequencies derived by measurement in Fig. 5(b) and analysis in Fig. 4(b) is due to the post-process deposition of SiO_2 to improve the shuttle engagement with beams, which is not included in simulations. Different voltage levels of piezoelectric beams are due to different levels of mechanical impact coupled from shuttle protrusions as a result of microfabrication non-idealities, such as residual stresses that release the beam tips at unequal heights.

To compare the system performance in Scenario 1 and Scenario 2, as described by Fig. 1, we measure the output voltage of one beam (B_1) in two different conditions, i.e. once when B_1 is plucked simultaneously with the beam on the opposite side (B_2) for Scenario 1, and then for Scenario 2 when B_1 is the only beam plucked by the actuator. This ensures that the mechanical input is divided between the two beams for Scenario 1, whereas for Scenario 2 it is applied to one beam only. In order to adjust the shuttle so that it impacts either a single beam or two beams together, a dc voltage is applied that moves the shuttle out-of-plane and pluck the beam tips at different heights. Hence, the random input is applied to the actuator with two different dc biases, which is adjusted by visually inspecting the beam tip under microscope.

The bandlimited Gaussian noise data file is generated in MATLAB and supplied through an arbitrary signal generator to the electrothermal actuator. Measurements are carried out by dc Signal Analyzer from B_1, and the results show an approximately 4dBVrms higher voltage output for Scenario 2 compared with Scenario 1. This is in agreement with the higher energy output expected for the proposed TDM technique.

IV. CONCLUSION

Existing frequency up-conversion techniques scavenge energy from the available inputs at a very small interval of input time period allowing the rest of period being wasted. This work presents a new TDM approach that is capable of increasing the energy harvester efficiency by exploiting the frequency up conversion of low frequency mechanical impacts at multiple instances over the low frequency time period. The prototype is implemented in Pz-MUMP, providing ease of manufacture and scale-up, with meander-like cantilever beams as EH elements. Theoretical analysis and experimental measurements support the higher efficiency of the proposed TDM approach.

REFERENCES

[1] A. G. Fowler, S. R. Moheimani, and S. Behrens, "Design and characterization of a 2-DOF MEMS ultrasonic energy harvester with triangular electrostatic electrodes," *IEEE Electron Device Lett.*, vol. 34, no. 11, pp. 1421-1423, 2013. doi:10.1109/Led.2013.2282815

[2] P. Johannisson, F. Ohlsson, and C. Rusu, "Impact-driven up-conversion in piezoelectric MEMS energy harvesters with pulsed excitation," in *J. Phys. Conf. Ser.*, 2018, vol. 1052, no. 1. doi:10.1088/1742-6596/1052/1/012106

[3] R. Kashyap, T. R. Lenka, and S. Baishya, "A Model for Doubly Clamped Piezoelectric Energy Harvesters With Segmented Electrodes," *IEEE Electron Device Lett.,* vol. 36, no. 12, pp. 1369-1372, 2015. doi:10.1109/Led.2015.2496186

[4] P. Kodali, A. Krishna, R. Varun, M. Prasad, and S. Sambandan, "Segmented electrodes for piezoelectric energy harvesters," *IEEE Electron Device Lett.,* vol. 35, no. 4, pp. 485-487, 2014. doi:10.1109/Led.2014.2305447

[5] H. Liu, C. J. Tay, C. Quan, T. Kobayashi, and C. Lee, "A scrape-through piezoelectric MEMS energy harvester with frequency broadband and up-conversion behaviors," *Microsystem technologies,* vol. 17, no. 12, pp. 1747-1754, 2011. doi:10.1007/s00542-011-1361-4

[6] A. Mohammadi, N. C. Karmakar, and M. R. Yuce, "A post-fabrication selective magnetic annealing technique in standard MEMS processes," *Appl. Phys. Lett.,* vol. 109, no. 22, p. 221906, 2016. doi:10.1063/1.4971262

[7] M. Ferrari, M. Bau, F. Cerini, and V. Ferrari, "Impact-Enhanced Multi-Beam Piezoelectric Converter for Energy Harvesting in Autonomous Sensors," *26th European Conference on Solid-State Transducers, Eurosensor 2012,* vol. 47, pp. 418-421, 2012. doi:10.1016/j.proeng.2012.09.173

[8] S. Adhikari, M. Friswell, G. Litak, and H. H. Khodaparast, "Design and analysis of vibration energy harvesters based on peak response statistics," *Smart Mater. Struct.,* vol. 25, no. 6, p. 065009, 2016. doi:10.1088/0964-1726/25/6/065009

[9] N. Khovanova and I. Khovanov, "The role of excitations statistic and nonlinearity in energy harvesting from random impulsive excitations," *Appl. Phys. Lett.,* vol. 99, no. 14, p. 144101, 2011. doi:10.1063/1.3647556

[10] G. Litak, M. Friswell, and S. Adhikari, "Magnetopiezoelastic energy harvesting driven by random excitations," *Appl. Phys. Lett,* vol. 96, no. 21, p. 214103, 2010. doi:10.1063/1.3120279

[11] A. Cowen, G. Hames, K. Glukh, and B. Hardy. PiezoMUMPs. ™. Design. Handbook a MUMPs® process [Online].

[12] A. Mohammadi, M. R. Yuce, and S. O. R. Moheimani, "Frequency Modulation Technique for MEMS Resistive Sensing," *IEEE Sens. J.,* vol. 12, no. 8, pp. 2690-2698, 2012. doi:10.1109/Jsen.2012.2198807